Energetics and electronic structure of stacking faults in ZnO

Yanfa Yan, G. M. Dalpian, M. M. Al-Jassim, and Su-Huai Wei
National Renewable Energy Laboratory, Golden, Colorado 80401, USA
(Received 7 May 2004; published 19 November 2004)

The energetics and electronic structures of basal-plane stacking faults in wurtzite (WZ) ZnO are studied using first-principles density-functional total energy calculations. All the basal-plane stacking faults are found to have very low formations energies. They also introduce a downward shift at the conduction-band minimum (CBM). However, plane-averaged charge densities of the CBM state reveal that the CBM states are not very localized, indicating that these stacking faults should be electronically inert. The high concentration of these stacking faults can result in embedded zinc-blende (ZB) ZnO surrounded by WZ materials. The WZ/ZB interface exhibits a type-II lineup with $\Delta E_V \approx 0.037$ eV and $\Delta E_C \approx 0.147$ eV.

DOI: 10.1103/PhysRevB.70.193206 PACS number(s): 61.72.Nn, 61.72.Yx, 61.72.Ji

ZnO has long been recognized as a useful material for optically transparent conducting layers in displays and photovoltaic devices.[1,2] Recently, it has attracted more attention because, like other wide-band-gap II-VI semiconductors, it could be an important material for next-generation short-wavelength optoelectronic devices such as low-cost light-emitting diodes (LEDs) and lasers, transparent *p-n* junctions, large-area flat-panel displays, and solar cells.[3–7] So far, most ZnO thin films are grown on mismatched substrates such as Al_2O_3 or SiC and contain a high density of extended defects.[8] Extended defects are known to play an important role in electronic and mechanical properties of semiconductors. For example, these defects may introduce electrically active energy levels in the energy gap.[9,10] In that case, the quantum efficiencies and device lifetime can be affected. Thus, it is important to know whether the extended defects are active or inert in ZnO thin films. So far, only the effects of inversion domain boundaries have been investigated.[11]

In II–VI semiconductor compounds, basal-plane stacking faults are one of the main types of extended defects. High-resolution transmission electron microscopy has observed such stacking faults even in ZnO films epitaxially grown on ZnO substrates.[12] In this paper, we present first-principles total-energy calculations on the atomic and electronic structures and formation energies of basal-plane stacking faults in WZ ZnO. We find that all basal-plane stacking faults have very low formation energies. The electronic structure calculations reveal that the stacking faults introduce a downward shift at the conduction band minimum (CBM). However, the CBM states are not very localized, indicating that the stacking faults are electronically inert. The high concentration of these stacking faults can result in embedded ZB ZnO surrounded by WZ materials. We find that the WZ/ZB interface exhibits a type-II lineup with $\Delta E_V \approx 0.037$ eV and $\Delta E_C \approx 0.147$ eV.

ZnO normally possesses a WZ structure, which can be described by the stacking of close-packed double layers of (0001) planes in the [0001] direction. The normal, perfect stacking sequence is …AaBbAaBb… . The perfect ZB structure can be described by the stacking sequence of …AaBbCcAaBbCc… . Here each letter represents a stacking plane. The upper-case and lower-case letters indicate Zn and O planes, respectively. The letters Aa, Bb, and Cc indicate three possible projected positions of the atoms. In the WZ structure, the two neighboring planes of every stacking plane are at the same position. In this case, Zn-O bonds in each stacking plane are called hexagonal bonds. In the ZB structure, the two neighboring planes of every stacking plane are at different positions. In this case, Zn-O bonds are called cubic bonds. The WZ structure contains only hexagonal bonds, whereas the ZB structure contains cubic bonds only.

A mistake induced to the perfect WZ stacking sequence will result in a basal-plane stacking fault in WZ ZnO. We study four types of basal-plane stacking faults proposed by Stampfl and Van de Walle[13] for stacking faults in WZ III-V nitrides. Figures 1(a)–1(c) show the structures for the so-called type-I, type-II, and type-III stacking faults. The type-I stacking faults contain one violation of the stacking rule, resulting in a stacking sequence: …AaBbAaBb|CcBbCcBb… . The symbol "|" indicates the position where the violation of the stacking rule starts. This stacking fault introduces one cubic bond in the stacking sequence, as indicated by the white arrow. The type-II stacking faults contain two violations of the stacking rule, giving a stacking sequence as …AaBbAaBb|CcAaCcAa… . It introduces two connected cubic bonds, as indicated by two white arrows. The type-III stacking faults contain a double-layer at the wrong position, leading to a stacking sequence as …AaBbAaBb|Cc|BbAaBb… . The two symbols "|" indicate the "wrong" double layer. It introduces two but separated cubic bonds at the interface. Figure 1(d) shows the structure of the extrinsic stacking faults, which contain an additional double layer inserted in the midst of the normal stacking sequence, resulting in a stacking sequence as …AaBbAaBb|Cc|AaBbAaBb… . The two symbols "|" indicate the additional double layer. It introduces three connected cubic bonds.

Our calculations on the total energy and electronic structure of stacking faults are based on the density-functional theory, using the Vienna *ab initio* Simulation Package (VASP).[14] We used the local density approximation for the exchange correlation, and ultrasoft Vanderbilt-type pseudopotentials[15] as supplied by Kresse and Hafner.[16] Because the formation energies for stacking faults are usually very small in most II-VI semiconductors, care must be taken to obtain accurate results. The Zn 3*d* electrons were treated

 ©2004 The American Physical Society

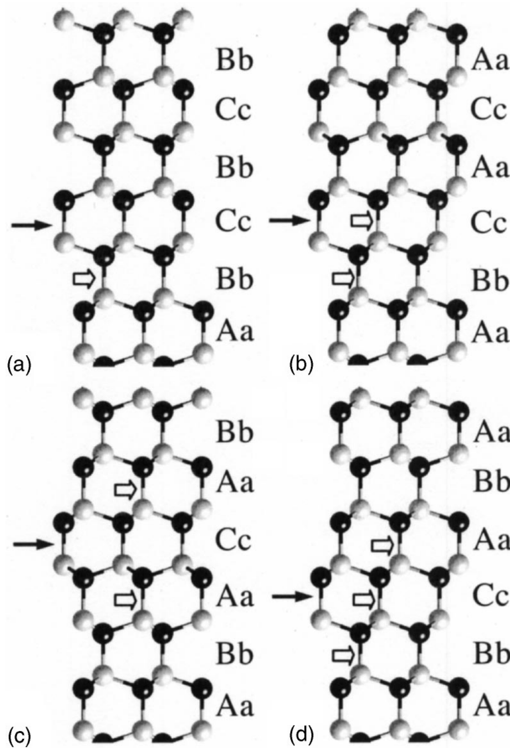

FIG. 1. Atomic structures of four types of basal-plane stacking faults in ZnO: (a) type I, (b) type II, (c) type III, and (d) extrinsic. The black balls indicate O atoms and gray balls denote Zn atoms. The arrows indicate the position of stacking faults.

as part of the valance band. Careful energy convergence tests showed that an energy cutoff of 360 eV is sufficient. The lattice constant was determined under this energy cutoff and was used for the supercell calculations. In all defect calculations, all atoms were allowed to relax to reach the minimum energies until the Hellmann-Feynman forces acting on them became less than 0.02 eV/Å. The band offsets between WZ ZnO and ZB ZnO were calculated using the WIEN 2K full potential linearized augmented plane wave code.[17] For the exchange and correlation potential, we used the generalized gradient approximation (GGA) of Perdew and Wang.[18]

The formation energies of the stacking faults are calculated using the supercell model.[19] To reduce the systematic error, a reference WZ supercell with an identical size and number of double layers is used. The same cutoff energy and the k-point grid were used for the supercells with or without the stacking fault. Because of these restrictions, we chose only supercells that have an even number of double layers and contain only equivalent stacking faults. For the type-I and type-III stacking faults, we used ten-double layer supercells to model their structures. The type-I supercell contains two equivalent stacking faults, whereas the type-III supercell contains only one. To model the type-II and extrinsic stacking faults, we built supercells contain 14 double layers. The type-II supercell has three equivalent stacking faults, whereas the supercell with an extrinsic stacking fault has two equivalent ones. Convergence checks for type-I and type-III stacking faults were carried out using 20 and 22 double-layer supercells. We found that the formation energies were lowered by less than 3 meV.

The formation energy of the stacking faults is obtained as

$$E_f = (E_{\mathrm{tot}}(\mathrm{defect}) - E_{\mathrm{tot}}(\mathrm{ref}))/(nS), \tag{1}$$

where E_{tot}(defect) is the total energy of the supercell containing stacking faults, E_{tot}(ref) is the total energy of the reference bulk WZ supercell, S is the fault area for a single planar defect in the supercell, and n is the number of stacking faults in the supercell.

Our calculated formation energies for type-I, type-II, type-III, and extrinsic stacking faults are 15, 31, 31, and 47 meV/(unit-cell area). The conversion factor from meV/(unit-cell area) to erg/cm^2 (or mJ/m^2) is 1.79. The formation energies are smaller for the type-I stacking fault, but larger for the extrinsic stacking. The formation energies are found to be proportional to the number of cubic bonds at the stacking faults [about 15±2 meV/(unit-cell area) per cubic bond]. This result suggests that the contribution to the stacking fault energy is quite local in ZnO, and can be obtained by simply counting on the number of cubic bonds at the stacking fault. Our calculated stacking fault energies are comparable to that in GaN and InN, but smaller than that in AlN.[13] However, these values are significantly smaller compared to those in more covalent materials, e.g., 318 and 254 erg/cm^2 for the intrinsic and extrinsic stacking faults, respectively, in C.[20] These small formation energies indicate that basal plane stacking faults may form very easily by kinetics in ZnO.

We have also investigated the electronic structure of the four types of stacking faults. Because the stacking faults introduce cubic bonds or thin ZB layers embedded in the WZ ZnO lattice, we first investigated the band offsets between WZ ZnO and ZB ZnO. The valance band offsets $\Delta E_\nu^{\mathrm{WZ\text{-}ZB}}$ for ZnO in WZ and ZB structures is calculated using the standard approach.[21,22] In this approach, the valance band offset is given by

$$\Delta E_\nu^{\mathrm{WZ\text{-}ZB}} = \Delta E_{\mathrm{VBM},C}^{\mathrm{WZ}} - \Delta E_{\mathrm{VBM}',C'}^{\mathrm{ZB}} + \Delta E_{C,C'}. \tag{2}$$

Here $\Delta E_{\mathrm{VBM},C}^{\mathrm{WZ}} = E_{\mathrm{VBM}}^{\mathrm{WZ}} - E_C^{\mathrm{WZ}}$ is the core level-to-VBM energy separation for an isolated WZ structure. A similar expression exists for $\Delta E_{\mathrm{VBM}',C'}^{\mathrm{ZB}}$. $\Delta E_{C,C'} = E_C^{\mathrm{WZ}} - E_{C'}^{\mathrm{ZB}}$ is the difference in core level binding energy between each side of the

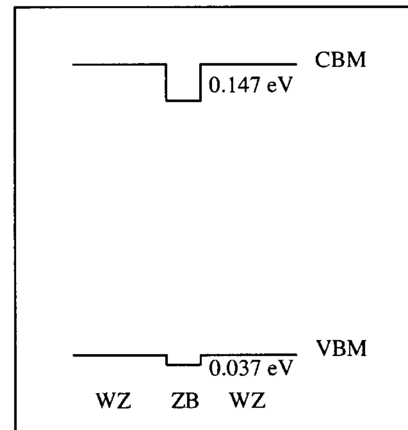

FIG. 2. A schematic plot of the band alignment of ZnO at the WZ/ZB/WZ regions.

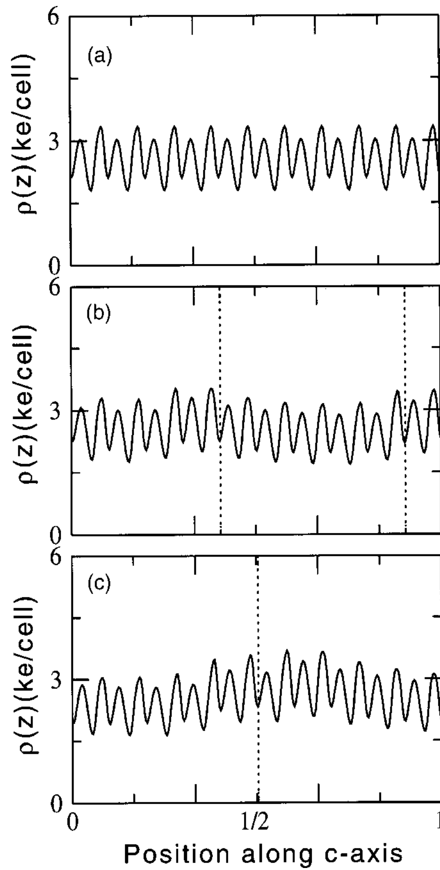

FIG. 3. Plane-averaged charge densities of CBM states of 10-double-layer supercells containing (a) perfect structure, (b) two equivalent type-I stacking faults, and (c) one type-III stacking fault. The dotted lines indicate the position of stacking faults.

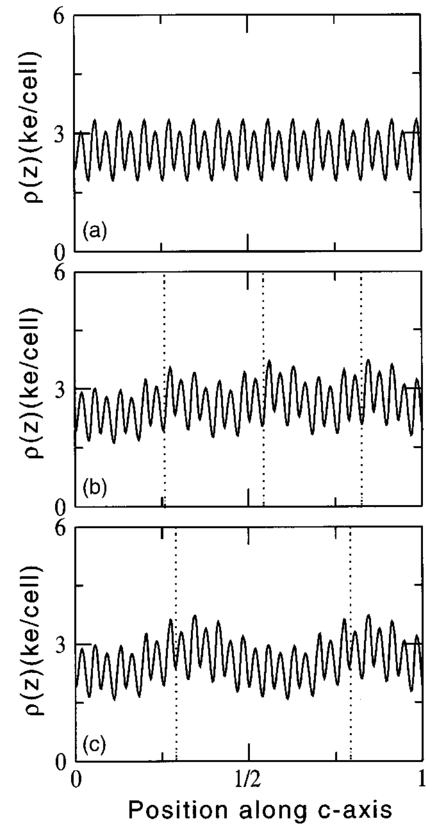

FIG. 4. Plane-averaged charge densities of CBM states of 14-double-layer supercells containing (a) perfect structure, (b) three equivalent type-II stacking faults, and (c) two extrinsic stacking faults. The dotted lines indicate the position of stacking faults.

WZ/ZB interface. It is calculated using a supercell with six double layers on each side, which is known to be sufficient for getting converged results.[23] We find that even though the WZ and ZB structures have a similar local structure, the core level difference $\Delta E_{C,C'}$ is not negligible in Eq. (2). Furthermore, because the WZ structure induces a spontaneous polarization, an average over the two polarities at the WZ/ZB interface is needed to calculate the core alignment across the interface.

The calculated valance band offset for WZ and ZB ZnO $\Delta E_v^{\text{WZ-ZB}}$ is 0.037 eV. The calculated WZ ZnO band gap is 0.11 eV larger than that for ZB ZnO. Thus, the conduction band offset for WZ and ZB $\Delta E_c^{\text{WZ-ZB}}$ is calculated to be 0.147 eV. Therefore, the band alignment is type II: the electronic states at the CBM are localized mainly in the ZB region, while those at the VBM are preferentially localized in the WZ region. The band alignment in mixed WZ/ZB/WZ regions is shown in Fig. 2. This band alignment indicates that the mixed WZ/ZB/WZ regions exhibit quantum-well-like features. Thus, carrier localization in the quantum-well-like regions is expected to affect the electronic and transport properties. For example, in a p-type ZnO film, the ZB well regions will behave like trap centers to the minority carriers (electrons), but diffusion barriers to the majority carriers (holes).

We found that all the stacking fault structures shown in Fig. 1 have a direct band gap at Γ. Their CBM are about 20 to 40 meV lower than that of the perfect crystal. But the shift in the VBM is negligible. These results are consistent with the band alignment shown in Fig. 2. To understand whether the downward-shifted CBM states are localized or not, we plotted the plane-averaged charge density of the CBM state along the c axis. Figure 3(a) shows the plane-averaged charge density of the CBM state for the ten-double-layer supercell with the perfect structure. Figures 3(b) and 3(c) show the plane-averaged charge densities for the ten-double-layer supercell with type-I and type-III stacking faults, respectively. We see that, as expected from the band alignment, the CBM is slightly more localized near the stacking faults. However, the localization effect is very weak due to the small CBM band offset and the small effective mass at the CBM.

Figure 4(a) shows the plane-averaged charge density of the CBM for the 14-double-layer supercell with the perfect structure. Figures 4(b) and 4(c) show the plane-averaged charge densities for the 14-double-layer supercell with type-II and extrinsic stacking faults, respectively. The supercell shown in Fig. 4(b) contains three equivalent stacking faults, whereas the supercell shown in Fig. 4(c) contains two equivalent stacking faults. The positions of the stacking

faults are indicated by the dotted lines. Again, we see that the CBM states are slightly more localized near the stacking faults, but the localization effect is very weak.

In conclusion, we have studied the atomic structure, energetics, and electronic structure of basal plane stacking faults in WZ ZnO by first-principles total-energy calculations. We found that all basal-plane stacking faults have very low formation energies, indicating the high density of stacking faults that may form in ZnO grown on mismatched substrates. These stacking faults induce a downward shift of the CBM. However, the CBM states are not very localized, indicating that the stacking faults are electronically inert. In the high concentration of stacking faults regions, embedded zinc-blende ZnO surrounded by WZ materials will form. We found that the WZ/ZB interface exhibits a type-II lineup with $\Delta E_V \approx 0.037$ eV and $\Delta E_C \approx 0.147$ eV.

The *ab initio* total-energy and molecular dynamics package, Vienna *ab initio* simulation package (VASP), was developed at the Institute für Theoretische Physik of the Technische Universit¨t Wien. This research was supported by the U.S. Department of Energy under Contract No. DE-AC36-99GO 10337, and used resources of the National Energy Research Scientific Computing Center, which is supported by the Office of Science of the U.S. Department of Energy under Contract No. DE-AC03-76SF00098.

[1] J. R. Tuttle, M. A. Contreras, T. J. Gillespie, K. R. Ramananthan, A. L. Tennant, J. Keane, A. M. Gabor, and R. Noufi, Prog. Photovoltaics **3**, 235 (1995).
[2] A. E. Delahoy and M. Cherny, Mater. Res. Soc. Symp. Proc. **426**, 467 (1996).
[3] H. J. Ko, Y. F. Chien, S. K. Hong, H. Wenisch, T. Yao, and D. C. Look, Appl. Phys. Lett. **77**, 3761 (2000).
[4] X. L. Guo, J. H. Choi, H. Tabata, and T. Kawai, Jpn. J. Appl. Phys., Part 2 **40**, L177 (2001).
[5] R. L. Hoffman, B. J. Norris, and J. F. Wager, Appl. Phys. Lett. **82**, 733 (2003)
[6] Y. R. Ryu, S. T. Lee, and H. W. White, Appl. Phys. Lett. **83**, 87 (2003).
[7] H. Ohta, H. Mizoguchi, M. Hirano, S. Narushima, T. Kamiya, and H. Hosono, Appl. Phys. Lett. **82**, 823 (2003).
[8] D. Gerthsen, D. Litivinov, Th. Gruber, C. Kirchner, and A. Waag, Appl. Phys. Lett. **81**, 3972 (2002).
[9] H. Iwata, U. Lindefelt, S. Oberg, and P. R. Briddon, Phys. Rev. B **65**, 033203 (2003).
[10] H. Iwata, U. Lindefelt, S. Oberg, and P. R. Briddon, J. Appl. Phys. **93**, 1577 (2003).
[11] Y. Yan and M. M. Al-Jassim, Phys. Rev. B **69**, 085204 (2004).
[12] X. L. Guo, J. H. Choi, H. Tabata, and T. Kawai, Jpn. J. Appl. Phys., Part 2 **40**, L177 (2001).
[13] C. Stampfl and C. G. Van de Walle, Phys. Rev. B **57**, R15052 (1998).
[14] G. Kresse and J. Hafner, Phys. Rev. B **47**, 558 (1993); **49**, 14 251 (1994); G. Kresse and J. Furthmüller, *ibid.* **54**, 11 169 (1996).
[15] D. Vanderbilt, Phys. Rev. B **41**, 7892 (1990).
[16] G. Kresse and J. Hafner, J. Phys.: Condens. Matter **6**, 8245 (1994).
[17] P. Blaha, K. Schwarz, G. K. H. Madsen, D. Kvasnicka, and J. Luitz, *WIEN 2K, An Augmented Plane Wave + Local Orbitals Program for Calculating Crystal Properties* (Karlheinz Schwarz, Techn. Universitat Wien, Austria, 2001). ISBN 3-9501031-1-2.
[18] J. P. Perdew and Y. Wang, Phys. Rev. B **33**, 8800 (1986).
[19] J. E. Northrup, J. Neugebauer, and L. T. Romano, Phys. Rev. Lett. **77**, 103 (1996).
[20] P. Käckell, J. Furthmüller, and F. Bechstedt, Phys. Rev. B **58**, 1326 (1998).
[21] S.-H. Wei and A. Zunger, Appl. Phys. Lett. **72**, 2011 (1998).
[22] S.-H. Wei and S. B. Zhang, Phys. Rev. B **62**, 6944 (2000).
[23] S.-H. Ke, K.-M. Zhang, and X.-de Xie, J. Phys.: Condens. Matter **8**, 10209 (1996).